

Supplementary data

Polymer/silica nanocomposite micro-objects as a key point for the silica-to-polymer shape replica

Patrizia Valsesia, Mario Beretta, Silvia Bracco, Angiolina Comotti, and Piero Sozzani*

*Materials Science Department, University of Milano-Bicocca and INSTM,
via R. Cozzi 53, 20125 Milano, Italy. E-mail: piero.sozzani@mater.unimib.it*

Figure 1. Energy-dispersive X-ray microanalysis of silica, nanocomposite and polymer

Figure 2. Powder X-ray diffraction patterns of silica and nanocomposite

Figure 3. ^{13}C MAS CP NMR spectra of polymethylmethacrylate and polystyrene nanocomposite.

Figure 4. SEM micrographs of selected single nanocomposite micro-objects.

Figure 5. TEM images of the silica micro-objects

Figure 6. TEM images of the polystyrene nanocomposite micro-objects

Figure 7. TEM images at different enlargements of the fully polymer micro-objects

Figure 8. Gel Permeation Chromatography plot of polystyrene micro-objects

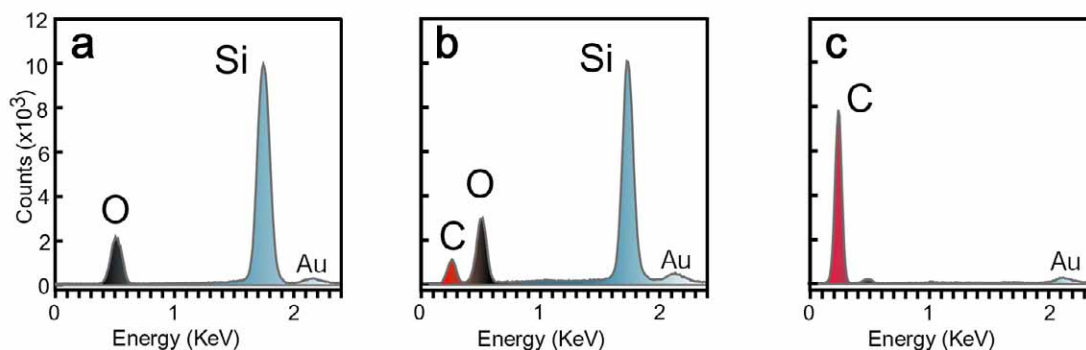


Figure 1. By energy-dispersive X-ray microanalysis it was possible to detect directly the composition of the objects obtained in the three different stages of the replica process. Starting from the fully silica particles (a), the obtainment of the nanocomposite is verified by the appearance of the carbon signal (b). Then, the apparent disappearance of the oxygen and silicon signals in the transformation from nanocomposite to polymer (c) gives evidence of the fully etching of the silica matrix.

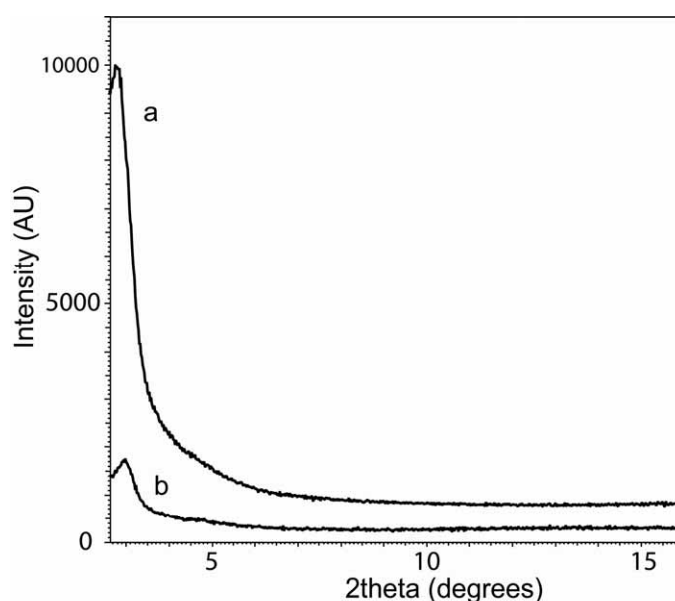


Figure 2. Powder X-ray diffraction patterns of (a) silica obtained under quiescent conditions and (b) nanocomposite particles recorded in the same conditions. The sharp peaks are due to the hexagonal arrangement of regular mesochannels of about 3 nm in diameter. The decrease in the peak intensity in the case of the nanocomposite, meaning a lower contrast in electron density, is a proof of the channels filled of polymer.

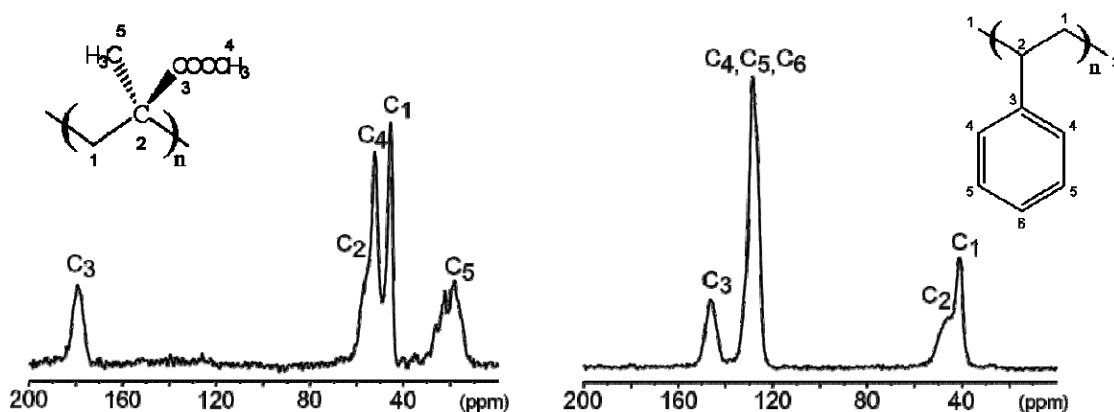


Figure 3. ^{13}C fast-MAS (15 KHz) CP NMR spectra of polymethylmethacrylate/silica nanocomposite (on the left) and polystyrene/silica nanocomposite (on the right).

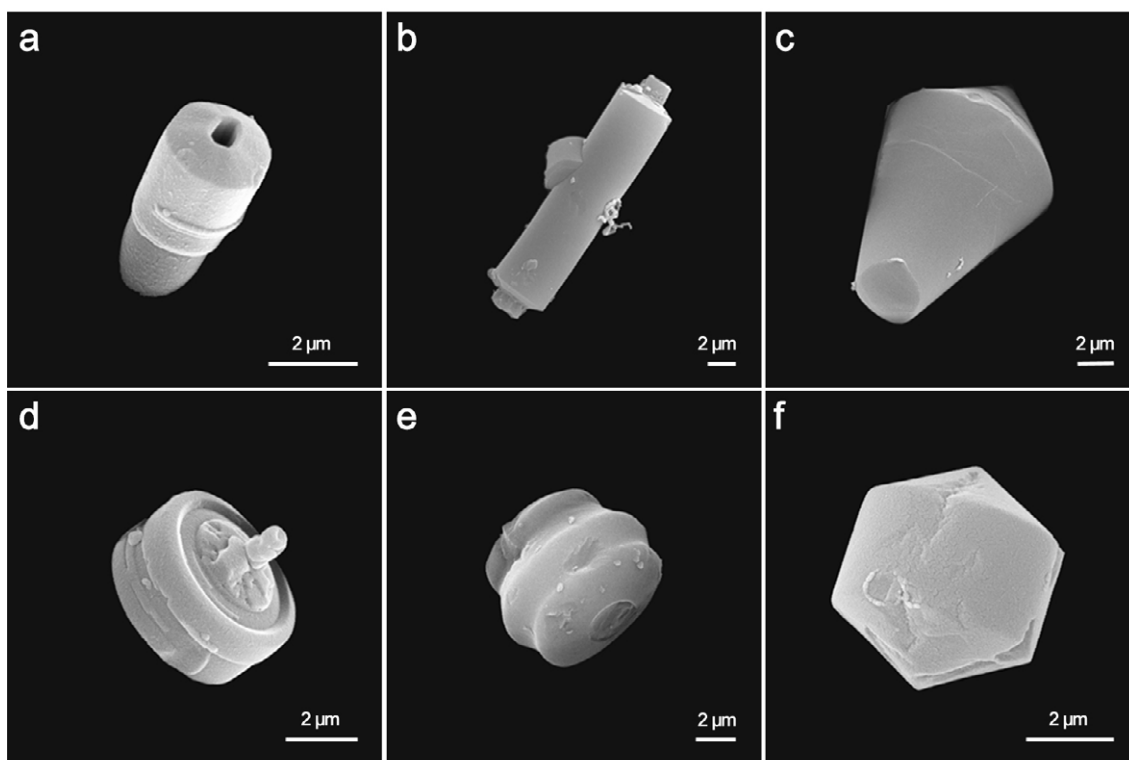


Figure 4. SEM micrographs of selected single nanocomposite objects recognized in the above samples. The nanocomposite adduct, that serves as a mediator for information transcription, assumes the architecture of a micrometric geometrical solid.

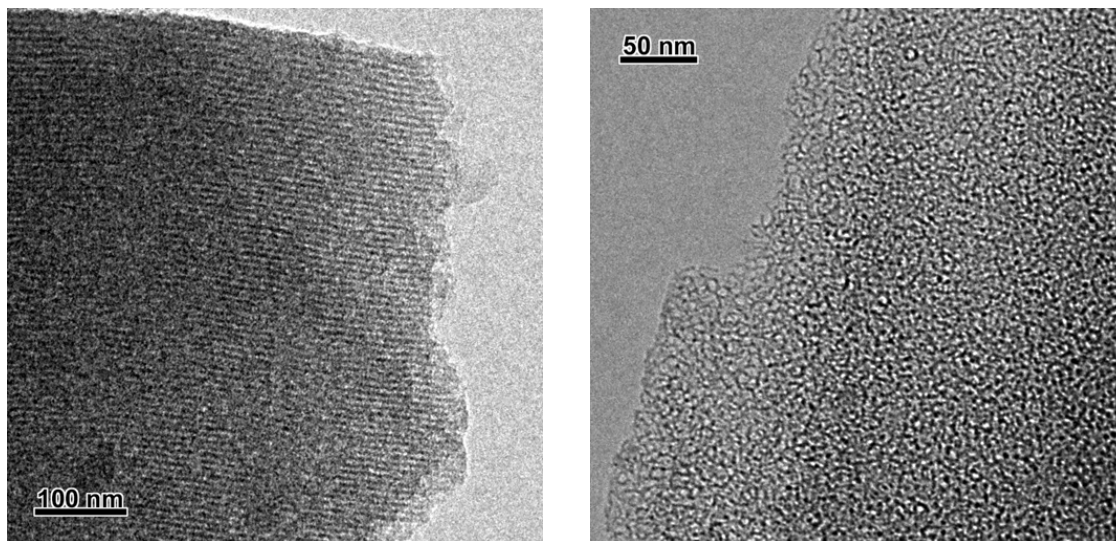


Figure 5. TEM images of the silica samples of MCM-41 nature, recorded with JEOL JEM-3010 (Acc.V=300kV, CL Aperture: 2nd largest, Spot size 3). Regularity of the pores but also interruptions of the channels and openings for the diffusion of the monomers are of interest.

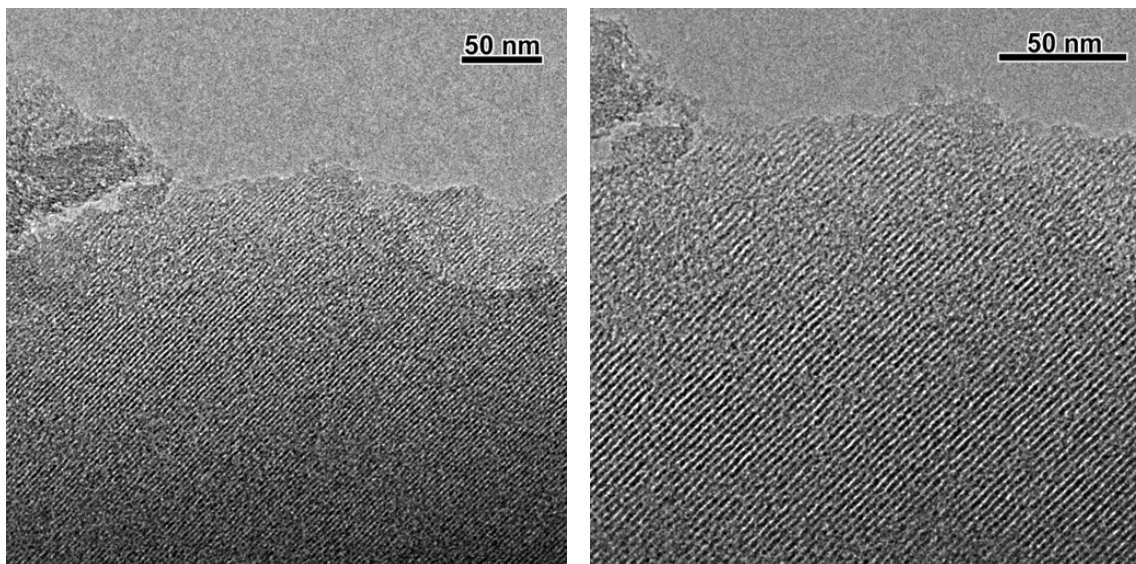


Figure 6. TEM images of the polystyrene nanocomposite particles, recorded with JEOL JEM-3010 (Acc.V=300kV, CL Aperture: 2nd largest, Spot size 3). The regularity of the pores, typical of the silica particles is maintained also in this stage.

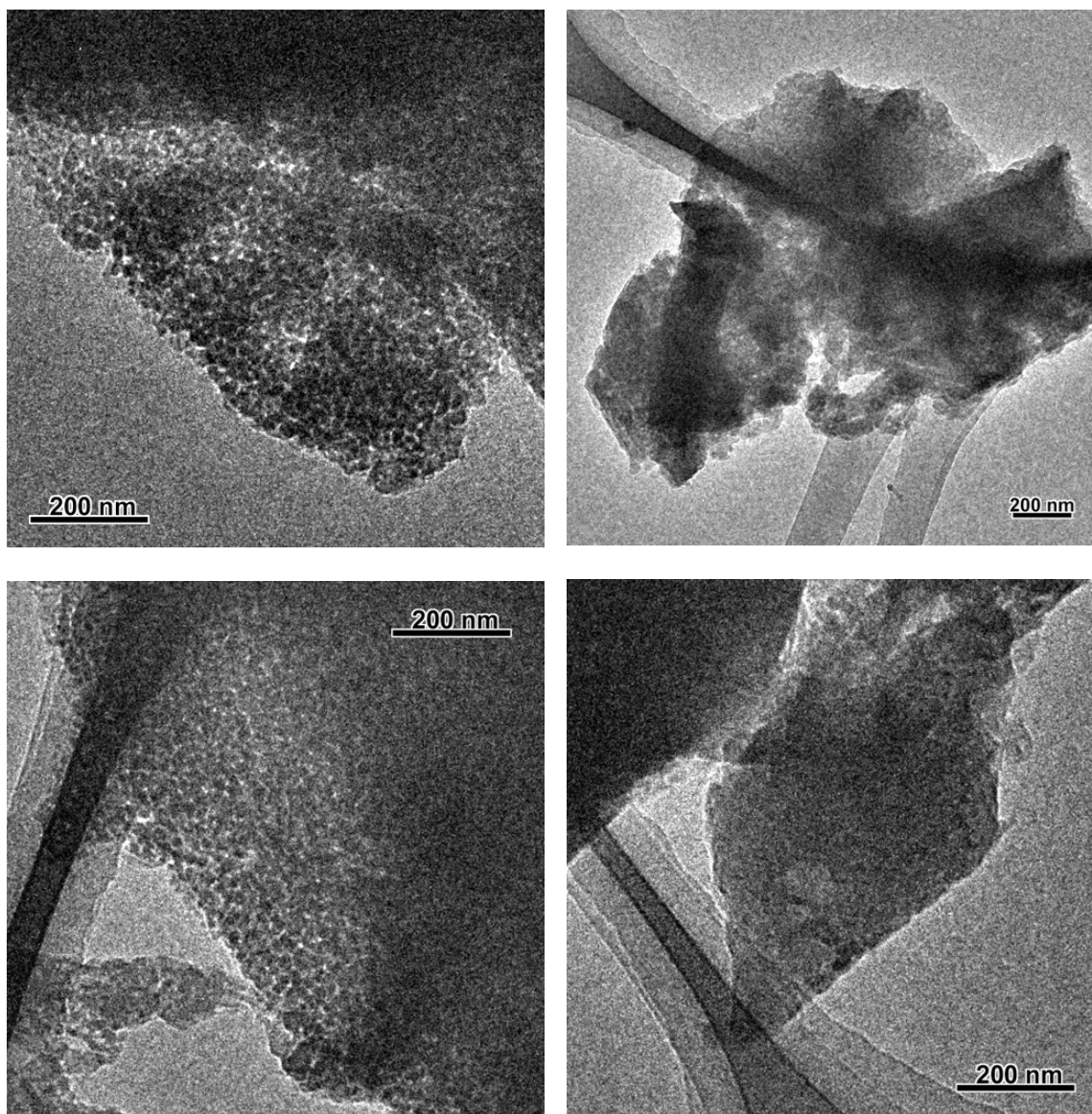


Figure 7. Some TEM images at different enlargements of the fully polymer objects, recorded with JEOL JEM-3010 (Acc.V=300kV, CL Aperture: 2nd largest, Spot size 5). The polymer sample containing a network of fibrils with a cross-section of about 5nm.

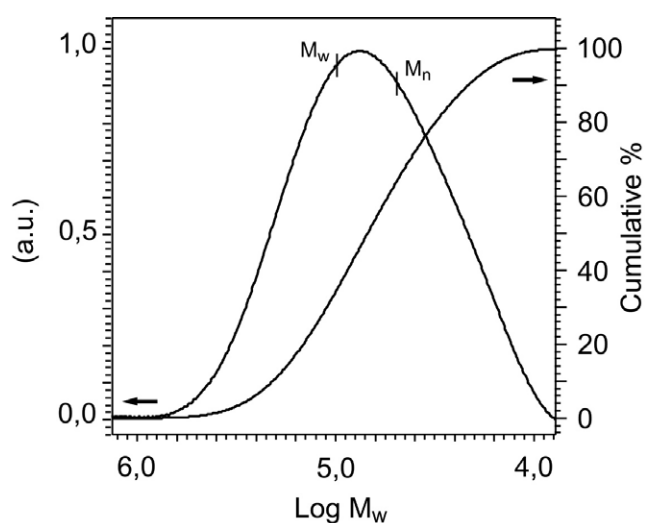


Figure 8. The number-average molecular mass M_n of polystyrene, the micro-objects are made of, valued by Gel Permeation Chromatography in tetrahydrofurane solution, is 48618 while the weight-average molecular mass M_w is 99200 and the polydispersity index $D=M_w/M_n$ is 2.04. In the case of polymethylmethacrylate objects M_w relative to polystyrene is 61300.